


RESEARCH

Open Access



Identification, validation and candidate gene analysis of major QTL for Supernumerary spikelets in wheat

Zhiqiang Wang^{1,2†}, Haojie Li^{1†}, Xinjian Zhou¹, Yuzhou Mou¹, Ying Zhang¹, Lang Yu¹, Xudong Chen¹, Fangkun Wu¹, Hong Zhou¹, Yu Lin¹, Caixia Li¹ and Yaxi Liu^{1*} 

Abstract

Background The number of spikelets per spike is a key trait that affects the yield of bread wheat (*Triticum aestivum* L.). Identification of the QTL for spikelets per spike and its genetic effects that could be used in molecular assistant breeding in the future.

Results In this study, four recombinant inbred line (RIL) populations were generated and used, having YuPi branching wheat (YP), with Supernumerary Spikelets (SS) phenotype, as a common parent. QTL (*QSS.sicau-2 A* and *QSS.sicau-2D*) related to SS trait were mapped on chromosomes 2 A and 2D through bulked segregant exome sequencing (BSE-Seq). Fourteen molecular markers were further developed within the localization interval, and *QSS.sicau-2 A* was narrowed to 3.0 cM covering 7.6 Mb physical region of the reference genome, explaining 13.7 – 15.9% the phenotypic variance. Similarly, the *QSS.sicau-2D* was narrowed to 1.8 cM covering 2.4 Mb physical region of the reference genome, and it explained 27.4 – 32.9% the phenotypic variance. These two QTL were validated in three different genetic backgrounds using the linked markers. *QSS.sicau-2 A* was identified as *WFZP-A*, and *QSS.sicau-2D* was identified a novel locus, different to the previously identified *WFZP-D*. Based on the gene expression patterns, gene annotation and sequence analysis, *TraesCS2D03G0260700* was predicted to be a potential candidate gene for *QSS.sicau-2D*.

Conclusion Two significant QTL for SS, namely *QSS.sicau-2 A* and *QSS.sicau-2D* were identified in multiple environments were identified and their effect in diverse genetic populations was assessed. *QSS.sicau-2D* is a novel QTL associated with the SS trait, with *TraesCS2D03G0260700* predicted as its candidate gene.

Keywords Wheat, QTL, BSE-seq, Supernumerary spikelets

[†]Zhiqiang Wang and Haojie Li contributed equally to this work.

*Correspondence:

Yaxi Liu

liuyaxi@sicau.edu.cn

¹State Key Laboratory of Crop Gene Exploration and Utilization in Southwest China, Triticeae Research Institute, Sichuan Agricultural University, Wenjiang, Chengdu 611130, China

²Chengdu Agricultural College, Chengdu 611130, Sichuan, China



Introduction

Wheat (*Triticum aestivum* L.) is one of the most important staple crops in the world, and estimates suggest that wheat production needs to increase 70% to fulfill food demand [1]. Therefore, maintaining food security and increasing yields to meet the higher demand of a growing global population has become a top priority for breeding programs [2].

Thousand grain weight (TGW), grain number per spike (GNS) and spike number per unit area are three major components of grain yield [3]. Among the above factors, the grain number per spike is affected by inflorescence architecture [4–6]. Plant inflorescences are small florets arranged on an axis, which can be divided into many types, such as racemes, spikes, corymbs, panicles etc. [7]. The wheat inflorescence is a spike, that usually consists of sessile spikelets arranged in opposite rows along the spike axis, each producing 3–5 florets [8]. Therefore, inflorescences, which determine the classification of Gramineae and the yield of food crops, have long been the subject of study of botanists and breeders [9]. In wheat germplasm resources, Supernumerary Spikelets (SS) is a special germplasm with many flowers and grains, which has the potential to improve the yield per unit area in wheat [10, 11]. SS can be divided into two types. One kind is called branched spikelets, where a spare spike extends on the stem node of the original spikelets and spikelets are born on it. The other type of spikelets is that the stem node does not extend, and two or more lateral spikelets are attached to the spike node, which is called supernumerary spikelets [12]. Identification of the QTL for spikelet number per spike (SNS) and its genetic effects that could be used in molecular assistant breeding in the future.

SNS is a complicated trait and controlled by quantitative trait loci (QTL) in wheat. To comprehend the molecular mechanisms that control this trait and to utilize it in breeding, QTL analyses have been conducted in wheat [13, 14]. Six QTL on chromosomes 1A, 2D, 3B, 6A, 7A, and 7D, were found to have dominant and epistatic effects [13]. Cui (2015) detected three QTL on chromosomes 2A, 5A, and 7B for SNS that were significant across multiple environments in two recombinant inbred lines (RILs) populations [15]. Four genomic regions affecting SNS on chromosomes 1A, 1B, 3A, and 7A were detected via a population of 191 F₉ RIL was developed from a cross of two winter cultivars Yumai8679 with Jing 411 [16]. Genotyping-by-sequencing (GBS) and the iSelect 9 K assay were used on a doubled-haploid (DH) soft red winter wheat population that showed a wide range of phenotypic variation for spike traits, and a major QTL *QSL.cz-1A/QFsn.cz-1A* which explained up to 30.9% of the phenotypic variation for spike length (SL) was identified [17]. In addition, *QFSN4B.4-17* responsible for SNS in multiple environments using a RIL population of 173

lines derived from a cross of the common winter wheat lines Shannong 01–35 and Gancheng 9411 was also identified previously [18].

To date, several genes affecting inflorescence structure and SNS have been identified and designated. For example, the HvMADS1 can directly regulate the expression of *HvCKX3* by binding to the promoter through a CArG-box domain, which affect the cytokinin homeostasis and inflorescence structure in barley [19]. In rice, APO1 interacts with APO2 to synergistically control cell proliferation in meristem and regulates panicle formation, and the overexpression of *APO1* or *APO2* has been associated with significantly increasing the spikelet number [4, 20, 21]. Several genes related to SNS were identified in wheat, including *WFZP* [22], *Ppd-1* [23], *FT2* [24], *WAPO1* [25], *Q* gene [26], and *Grain Number Increase 1* [27].

Although there are many reports about QTL related to wheat spikelet number, only few of QTL have been genetically verified, offering a foundation for fine mapping and map-based cloning. This has greatly restricted the dissection of the molecular mechanisms underlying spikelet number as well as improvement of spikelet number in wheat breeding. Thus, the identification and validation of novel QTL/genes for spikelet number is important. In this study, we used a RIL population (YC) derived from a cross between YuPi branching wheat (YP) and Chinese spring wheat (CS), to identify QTL associated with SS trait using a high-density genetic map and phenotypic data obtained from a multiple environmental trial, in different genetic backgrounds.

Materials and methods

Plant materials

The common parent YP is a bread wheat germplasm with the SS character [28, 29]. An RIL population generated by the single seed descent method from a cross YP × CS (YC population, 215 F₆/F₇ lines), was used for BSE-Seq and QTL mapping. Three RIL populations derived from the crosses YP × CM107 (YCM population, 132 F₆/F₇ lines), YP × CM104 (YJ population, 60 F₆/F₇ lines) and YP × 11N21 (NY2 population, 73 F₆/F₇ lines), were used to validate the QTL in different genetic backgrounds.

Phenotypic evaluation and statistical analysis

YC RIL population were planted in three environments: Chongzhou (CZ, 103° 38' E, 30° 32' N) in 2021–2022 (2022CZ), Chongzhou and Wenjiang (WJ, 103° 41' E, 30° 36' N) in 2022–2023 (2023CZ and 2023WJ). A randomized complete block design was adopted in all environments. YCM, YJ and NY2 populations were planted at Chongzhou in 2022–2023. Fifteen seeds of each family were planted in 1.5 m rows spaced 30 cm apart. Field management was performed according to

recommendations for wheat production. After maturity, five plants from the center rows were selected and used for phenotypic evaluation, including the number of SS per spike (NSS), SNS, TGW, GNS, grain weight per spike (GWS), grain length (GL), grain width (GW), flag leaf length (FLL) and flag leaf width (FLW). The SNS was determined by counting the total spikelets in the main spike, NSS was calculated by deducing the number of nodes per spike from SNS. GNS, GWS, GL and GW were measured by a Wanshan SC-G automatic seed test system (Hangzhou Wanshan Detection Technology Co., Ltd., CN). The TGW was calculated as 10-fold of the weight of 100 seeds measured with an electronic balance, in three replicates for each line [1].

Analysis of variance (ANOVA) for the NSS in each trial and Pearson correlations between variables were computed in SPSS v27 (IBM SPSS, Chicago, IL, USA). To minimize environmental effects, the best linear unbiased estimates (BLUE) for NSS in three replicates was calculated using SAS 8.1 (SAS Institute Inc., Cary, NC, USA). According to the method described by Smith, broad-sense heritability (h^2) across environments was estimated, according to the equation $h^2 = V_G / (V_G + V_{GE}/r + V_E)$, where V_G = genotypic variance, V_{GE} = genotype \times environment variance, r = number of replicates, and V_E = environmental variance. Student's t -tests ($P < 0.05$) were applied to compare lines classified by genotype [30, 31].

Bulked Segregant Analysis and Exome sequencing

Total genomic DNAs were isolated from young leaves of the tested cultivars and RILs using a CTAB method followed by RNase-A digestion [32]. Isolated DNA was quality checked by resolving on a 1% agarose gel electrophoresis and concentration was determined using a UV spectrometer [33, 34]. Two DNA pools were constructed by mixing equal amounts of DNA normalized to the concentration 100 ng/ μ L from 30 extreme SS (SS-pool) and 30 normal spike types (NS-pool), respectively. The DNA libraries were constructed through DNA fragmentation, end-repair, adaptor ligation, PCR and hybridization capture as previously described [35]. Curated sequence data was aligned to the CS reference genome sequence (RefSeq) v2.1 by BWA software [36]. The BCFtools software was used to detect and extract the single nucleotide polymorphism (SNP) and InDel [37]. The SNP and InDel were annotated using ANNOVAR, which mainly included different regions of the genome and different types of exon regions [38]. SNP-index methods were used to screen the SNP and InDel sites with candidate regions between the progeny mixed pools in this study [39–42]. To identify candidate regions associated with the SS trait, the Δ SNP-index of each locus was calculated by subtracting the SNP-index of the SS-pool from that of the NS-pool according to previous method [43]. To confirm the

results of Δ SNP-index, an algorithm was further performed to identify the SNPs and InDels associated with the SS trait using the equation reported previously [31, 40], and the absolute value of Δ (SNP-index) was used for Locally Weighted Scatterplot Smoothing (LOESS) to obtain the correlation threshold [2]. The greater the Δ SNP-index, the more likely the SNPs and InDels contribute to the trait of SS or is linked to a locus that controls the trait.

Marker development, genetic map construction and QTL identification

To validate the BSE-seq results and further narrow down the region, primers were designed to flank the sequences of the targeted SNPs using an online tool of the wheatomics platform (<http://wheatomics.sdau.edu.cn/PrimerServer/>). Polymorphic SNPs between YP and CS in the initial mapping region were converted to KASP markers following previously described methods [44]. The PCR for InDel primers was conducted in a 20 μ L reaction volume with 1.0 μ M primer mix, 2.5 ng/ μ L DNA and 1 \times Taq Master Mix (Vazyme Biotech, CN). PCR was performed using routine procedures, and the polyacrylamide gel (8%) electrophoresis was used for resolving amplified products [34]. The polymorphisms of the markers were confirmed by parental lines and some progenies.

Linkage mapping was conducted using JoinMap v4.0 [45]. The maximum likelihood mapping algorithm and Kosambi's function were used to determine the marker order and distance, respectively. QTL analysis of SS trait was performed by Interval Mapping (IM) with the software MapQTL v5.0 [46]. For each trial, a test of 1,000 permutations was performed to identify the LOD threshold corresponding to a genome-wide false discovery rate of 1% ($P < 0.01$).

QTL validation

For QTL validation, the NSS from all homozygous lines in each of the three RIL populations (YCM, YJ and NY2) were counted. Based on marker profiles, individuals in each population were grouped into two classes as described above, and the difference in the average spikelet number between these classes was used for measuring the QTL effects within each validation population. The Student's t -test was used to determine the significance in differences between the two groups in each population at $P < 0.05$.

Prediction of candidate genes for QTL

The physical interval of QTL was obtained by conducting a homolog search of the flanking markers against the Chinese Spring reference genome (IWGSC_Refseq v2.1), and the genes mapped to the region were identified. Further,

Table 1 Distribution of NSS in the YC population

Trait	Environment	Parents		Population			
		Mean of YP	Mean of CS	Range	Mean	SD	H ²
NSS	CZ2022	56.40**	0.00	0.00-36.60	5.00	8.10	
	WJ2023	65.80**	0.00	0.00-63.60	7.81	14.51	
	CZ2023	62.20**	0.00	0.00-58.20	5.82	10.91	
	BLUE	57.31**	0.21	0.21-53.0	6.42	10.74	0.96
SNS	BLUE	70.51**	26.82	16.94-73.55	30.17	10.36	0.88
GWS	BLUE	3.87**	1.91	1.52-2.93	2.01	0.21	0.55
TGW	BLUE	37.49**	27.92	23.38-43.10	34.10	3.78	0.76
GNS	BLUE	108.07**	62.71	41.56-85.34	59.33	7.94	0.62
GL/mm	BLUE	6.82**	5.24	6.54-9.16	7.97	0.40	0.87
GW/mm	BLUE	2.78	2.72	3.23-4.17	3.79	0.17	0.74
FLL/cm	BLUE	22.61**	25.12	18.20-29.54	22.49	2.04	0.70
FLW/cm	BLUE	1.84**	1.53	1.27-2.00	1.60	0.12	0.72

** indicate significant differences at $P < 0.01$. NSS, the number of SS per spike. SNS, spikelets number per spike. GNS, grain number per spike. GWS, grain weight per spike. TGW, thousand grain weight. GL, grain length. GW, grain width. FLL, flag leaf length. FLW, flag leaf width. BLUE, best linear unbiased estimator

**Fig. 1** Spike features of YuPi branching wheat (YP) and Chinese spring wheat (CS)

information on the genes were obtained from the wheatomics platform (<http://wheatomics.sdau.edu.cn/>). The expression values as transcripts per million (TPM) in roots, stems, leaves, spikes, and grain were obtained from

the GeneExpression of Wheatomics platform. Genes were annotated through BLAST against the corresponding protein sequences in rice and *Arabidopsis thaliana* on KOBAS v3.0 [47]. The total RNA was extracted by using the RNeasy plant mini kit (Qiagen, CN) from CS and YP at the correct stage, and the products after reverse transcription were used for quantitative RT-qPCR. The genomic DNA of parents was used to amplify candidate genes for sequence analysis.

Results

The NSS of YC RIL population in different environments

In the different environments, the NSS of CS remained stable at 0, while that of YP ranged from 56.4 to 65.8, with the NSS of YP being significantly ($P < 0.01$) higher than that of CS (Table 1; Fig. 1). The NSS trait in YC population was also observed in different environments, ranged from 0 to 63.6, and the broad-sense heritability was estimated as 0.96 (Table 1). The correlation coefficients between the different environments were all significant and ranged from 0.922 ($P < 0.01$) to 0.982 ($P < 0.01$) (Table 2). The BLUE values of SNS, GWS, TGW, GNS, GL, GW, FLL and FLW were shown in Table 1 and were used to assess the effect of SS QTL on these traits.

BSE-seq analysis

The results obtained from the exome capture sequencing of bulked segregants were compared with the CS reference genome v2.1. We use the Δ SNP-index algorithm to

Table 2 Correlation coefficients for the NSS in the YC population

repetition	CZ2022	CZ2023	WJ2023	BLUP
CZ2022	1			
CZ2023	0.922**	1		
WJ2023	0.922**	0.925**	1	
BLUE	0.965**	0.982**	0.973**	1

** indicate significant differences at $P < 0.01$

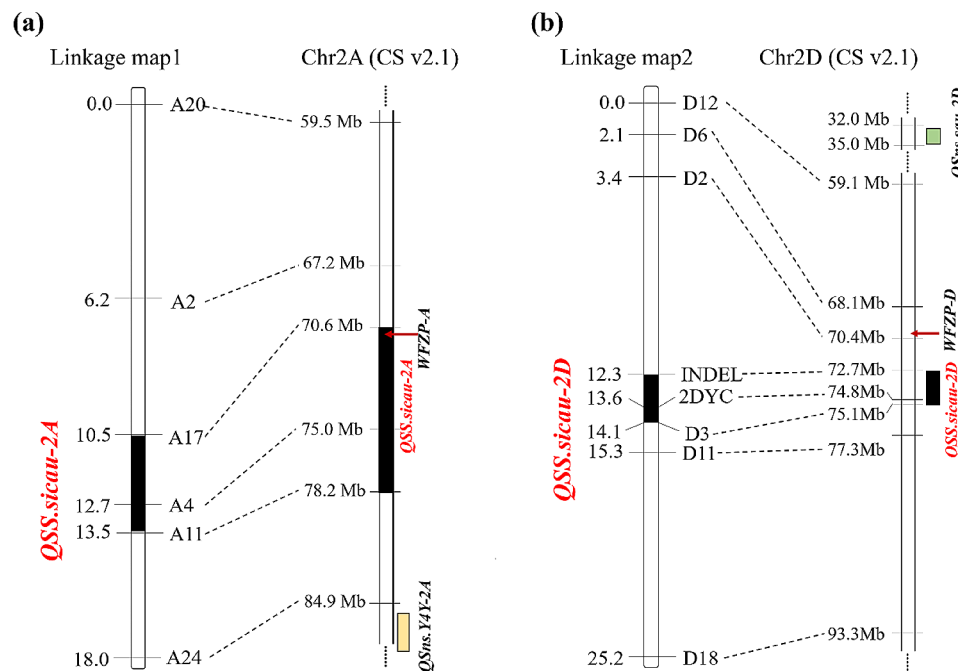


Fig. 2 Linkage map of chromosome 2 A and chromosome 2D. **(a)** Physical map of chr2A, with *QSS.sicau-2A* mapped on a region of the 3.0 cM genetic map. **(b)** Physical map of Chr2D, with *QSS.sicau-2D* mapped on a region of the 1.8 cM genetic map

Table 3 QTL analysis for SS in different environments and the BLUE datasets

QTL	Environment	Flanking markers	LOD	LOD Thre	PVE(%)	Add	Physical interval(Mb)
<i>QSS.sicau-2A</i>	CZ2022	A11, A17	7.9	3.2	15.5	3.72	70.6–78.2
	CZ2023	A11, A17	8.0	3.3	15.7	6.44	70.6–78.2
	WJ2023	A11, A17	6.9	3.2	13.7	4.62	70.6–78.2
	BLUE	A11, A17	8.1	3.4	15.9	4.90	70.6–78.2
<i>QSS.sicau-2D</i>	CZ2022	INDEL, D3	15.0	2.9	27.4	6.62	72.7–75.1
	CZ2023	INDEL, D3	15.3	2.9	27.8	8.69	72.7–75.1
	WJ2023	INDEL, D3	18.7	3.1	32.9	5.49	72.7–75.1
	BLUE	INDEL, D3	17.1	3.5	30.6	6.91	72.7–75.1

LOD, logarithm of odds. LOD Thre, the LOD threshold. PVE, phenotypic variation explained. Add, additive effect (positive values indicate that alleles from YP increased trait scores, and negative values indicate that alleles from CS increased trait scores). BLUE, best linear unbiased estimator

calculate the allele segregation of the SNPs and InDels between two extreme DNA pools. Δ SNP-index algorithm showed abundant candidate SNPs/InDels enriched on chromosome 2 A and 2D (Chr2A and Chr2D). Δ SNP-index greater than 95% confidence interval was selected as the threshold for screening [48]. A 16.3 Mb region of Chr2A (63.8–80.1 Mb) and a 9.1 Mb region of Chr2D (68.1–77.2 Mb) were identified as the candidate regions for SS trait (Figure S1).

Linkage map construction and QTL identification

To confirm the preliminarily identified genomic regions responsible for SS trait, SNPs and InDels in the target regions were converted into KASP and InDel markers, and were used for the construction of the genetic map. In total, 13 KASP markers and one InDel marker were used for the construction of the genetic maps. Six KASP

markers developed for Chr2A generated a linkage map spanning 18.0 cM, while seven KASP markers and one InDel marker developed for Chr2D generated a linkage map spanning 25.2 cM (Fig. 2, Table S1). The phenotypic data of SS trait evaluated in the three environments were used for QTL mapping. Two stable QTLs named *QSS.sicau-2A* and *QSS.sicau-2D* were detected in three environments and BLUE. *QSS.sicau-2A* located between A11 and A17, explained 13.7–15.9% of the phenotypic variance with the LOD values ranging from 6.9 to 8.1. *QSS.sicau-2D* located between INDEL and D3, explained 27.4–32.9% of the phenotypic variance with the LOD values ranging from 15.0 to 18.7 (Table 3). The favorable alleles of the two QTL were all contributed by YP.

Effects of supernumerary spikelet QTL in different genetic backgrounds

Three KASP markers (A4, D3, 2DYC) and one InDel marker (INDEL) were used to assess the effects of QTL on NSS in validation populations (A4 is linked to *QSS.sicau-2 A* and exhibits polymorphism across the three validation populations. INDEL, 2DYC and D3 are linked to *QSS.sicau-2D* and exhibit polymorphism in YJ, G2 and NY2 populations, respectively). In YJ population, the average NSS in homozygous “AA, DD” genotype was 17.71, that was significantly ($P < 0.01$) increased than that in homozygous “aa, dd”, “AA, dd” and “aa, DD” genotypes. Similarly, in G2 and NY2 populations, the average NSS in homozygous “AA, DD” genotypes were 15.75 and 14.52, respectively, that significantly ($P < 0.01$) increased than that in other three homozygous genotypes (Fig. 3).

Candidate gene prediction

According to the CS genome (IWGSC Refseq v2.1), *QSS.sicau-2 A* was located between 70.6 Mb and 78.2 Mb on Chr2A, and 91 high-confidence genes, including *WFZP-A* (*TraesCS2A03G0239400*) spanned the region. Sequence analysis of the *WFZP-A* (Table S2), revealed a 4-bp deletion in *WFZP-A* resulting a frame-shift in YP (Figure S2, Table S3), and the variation type is consistent with Zang734 [49]. These results suggest that *WFZP-A* is likely responsible for *QSS.sicau-2 A*.

QSS.sicau-2D was mapped between 72.7 Mb and 75.1 Mb on Chr2D, revealing 34 high-confidence genes in the region (Table S4). Eight spike/grain-specific genes were identified by gene expression of WheatOmics (<http://202.194.139.32/expression/index.html>), that might probably be involved in spike growth and development (Table S5, Figure S3). Exome sequencing data of YP reveal one T to A substitution which converts the codon (TAT) to a translational stop codon (TAA) in *TraesCS2D03G0260700* (Fig. 4). Additionally, we examined the coding sequences of the known branching gene *WZFP-D*

(*TraesCS2D03G0248500*, chr2D: 69,940,372.69,941,615). No sequence variation between YP and CS was identified for *WZFP-D*, and no significant difference ($P > 0.05$) in gene expression in YP and CS (Figure S4, Table S3).

Effects of *QSS.sicau-2 A* and *QSS.sicau-2D* on yield-related traits

Two QTL, *QSS.sicau-2 A* and *QSS.sicau-2D*, were identified in YC population. Their effects on the yield-related traits were analyzed by linking markers. The YC population was divided into four genotypes of “aa, dd”, “AA, dd”, “aa, DD” and “AA, DD” by molecular markers. The SNS, GNS and GWS of homozygous “AA, DD” genotypes were significantly higher than that of other three genotypes, the TGW, GL and GW of homozygous “AA, DD” genotypes were significantly lower than that of other three genotypes (Fig. 5a and f). Additionally, the FLL and FLW were not affected by *QSS.sicau-2 A* and *QSS.sicau-2D* (Fig. 5g and h).

Discussion

The complexity of the wheat genome combined with the fewer spikelet number mutants, hinder the identification of beneficial variants associated with spikelet number. To enhance the yield potential of wheat, breeders have tried to alter its sink capacity by modifying spike morphology [50]. The supernumerary spikelet (SS) character of bread wheat (*Triticum aestivum* L.) is an abnormal spike morphology with extra spikelets per rachis node. In some materials, the SS trait was unstable, and some environmental factors and photoperiod could affect the expression of *bh* gene for SS character [51, 52]. In this study, YP maintained SS trait in multiple environments, which provides an available germplasm resource for improving wheat spikelets.

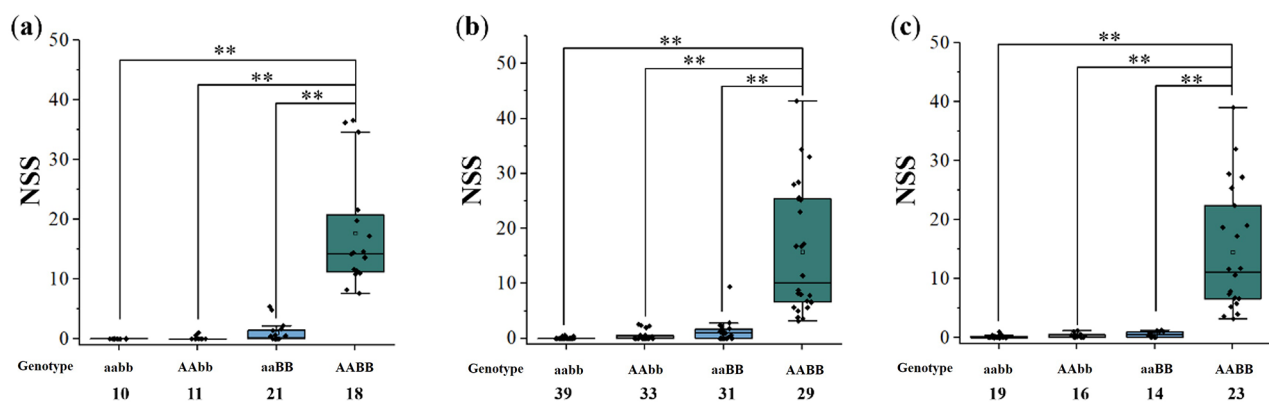


Fig. 3 The effects of *QSS.sicau-2 A* and *QSS.sicau-2D* on NSS in the validation populations. (a) YP/CM104 RIL population. (b) YP/CM107 RIL population. (c) YP/11N21 RIL population. ** indicate significance level at $P < 0.01$ by the Student's t-test. NSS, the number of SS per spike

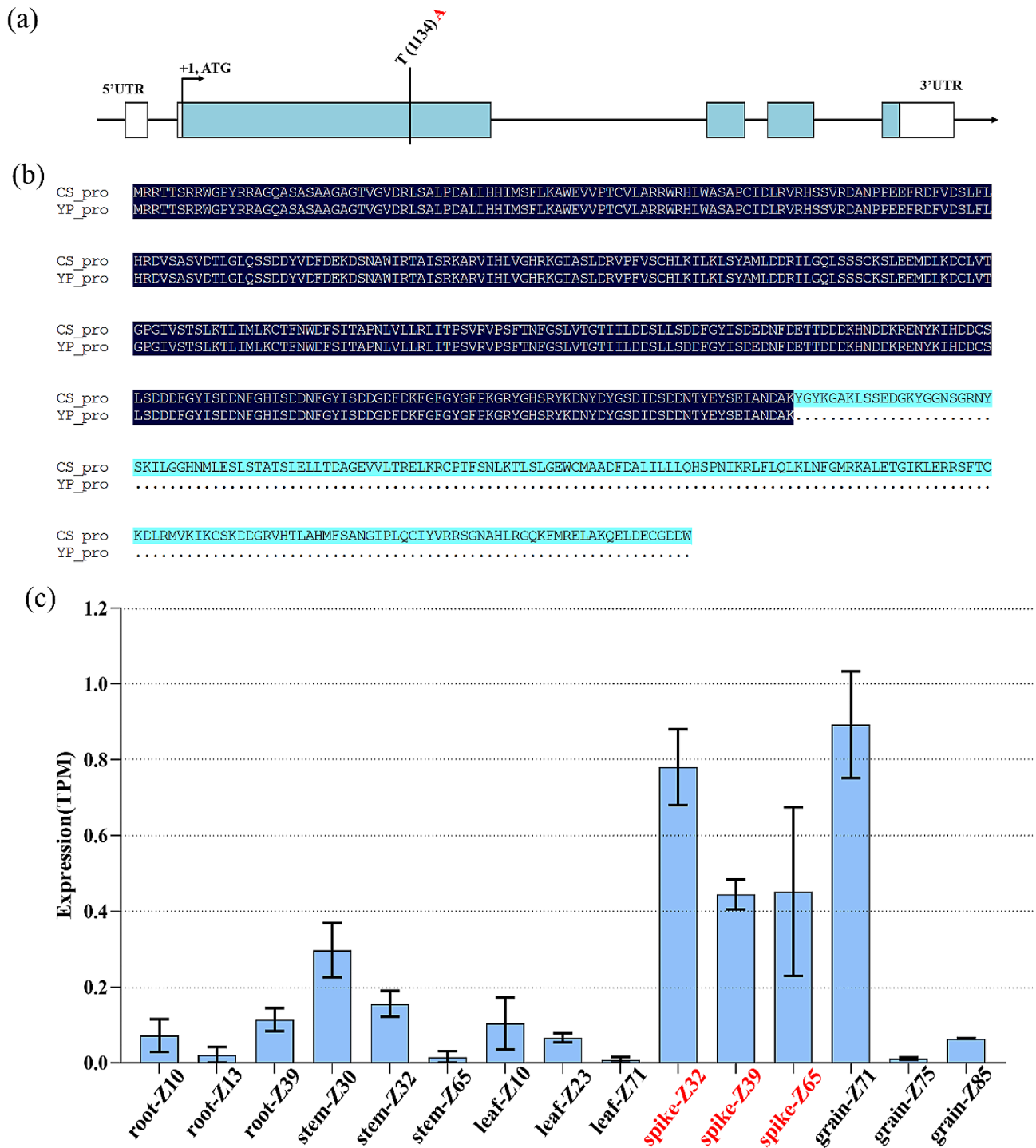


Fig. 4 Variation sequence and expression patterns of *TraesCS2D03G0260700*. (a) The nucleotide of YP and CS are shown in red and black, respectively. (b) The amino acid sequence encoded by the *TraesCS2D03G0260700* in YP and CS. (c) *TraesCS2D03G0260700* expression patterns in different tissues, the data (TPM value) were downloaded from the GeneExpression of WheatOmics (<http://wheatomics.sdau.edu.cn/>). Z10, first leaf through coleoptile. Z13, 3 leaves unfolded. Z23, main shoot and 3 tillers. Z30, pseudo stem erection. Z32, 2nd node detectable. Z39, flag leaf ligule/collar just visible. Z65, anthesis half-way. Z71, caryopsis water ripe. Z75, medium milk. Z85, soft dough

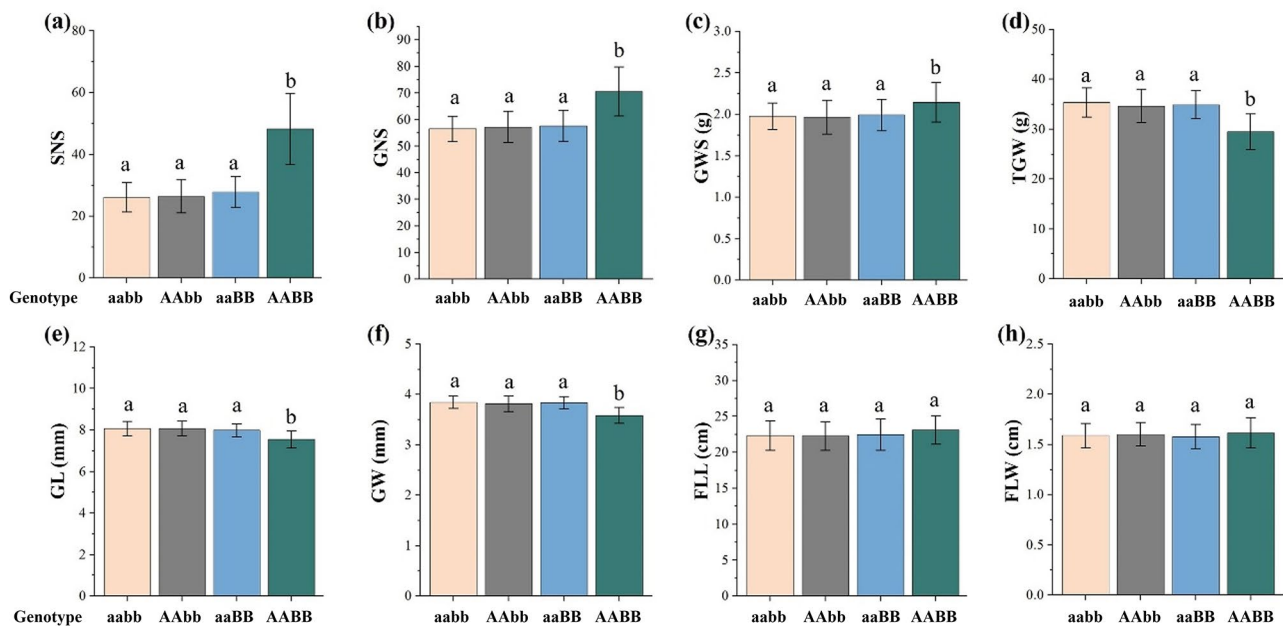


Fig. 5 Effects of *QSS.sicau-2A* and *QSS.sicau-2D* on grain traits and flag leaf. Bar pattern and significance analysis of (a) SNS, (b) GNS, (c) GWS, (d) TGW, (e) GL, (f) GW, (g) FLL and (h) FLW. Each bar shows mean \pm SD. Different letters indicate significance level at $P < 0.05$ by the Tukey's test. SNS, spikelets number per spike. GNS, grain number per spike. GWS, grain weight per spike. TGW, thousand gain weight. GL, grain length. GW, grain width. FLL, flag leaf length. FLW, flag leaf width

Comparison of QTL identified for wheat spikelet number with previous studies

In recent years, many QTLs related to SNS have been widely reported and were mapped to all 21 chromosomes of wheat [14, 53–56]. *Qsns.Y4Y-2 A*, a QTL related to SNS, was detected in multiple environments and mapped between 85.6 Mb and 91.1 Mb [57]. Li [58] found one local cultivar YM44 that has SS phenotype, which was linked to the marker *Xwmc522* and *cf_d56* mapped on chromosome 2 A and 2D, respectively, and further confirmed that *WFZP-A* is the functional gene of chromosome 2 A that causes SS phenotype. In this study, we found that *WFZP-A* (Chr2A: 71,582,645.71,583,948) exists in the *QSS.sicau-2 A* (70.6–78.2 Mb) interval, and the similar variation existed in YP by the sequences analysis of *WFZP-A* in YP and CS (Figure S2). Therefore, we speculate that *WFZP-A* may be responsible for *QSS.sicau-2 A*.

In addition, several QTL controlling SNS trait have been reported on chromosome 2D in wheat. *Qsns.sau-2D* was mapped on chromosome arm 2DS flanked by the markers *AX-109,836,946* (32.8 Mb) and *AX-111,956,072* (34.4 Mb) [59]. Gene *Mrs1* on the short arm of chromosome 2D, that closely linked to *Xgwm 484* (50.6 Mb), and further identified the candidate gene *WFZP-D* (chr2D: 69,940,372.69,941,615) by homologous function annotation [22, 60]. In this study, *QSS.sicau-2D* was mapped to the genomic region of Chr2D between 72.7- and 75.1 Mb, and no overlap between the QTL interval associated with

SNS and indicating *QSS.sicau-2D* may be a novel QTL for SS trait.

Potential candidate genes for *QSS.sicau-2D*

To screen the candidate gene for *QSS.sicau-2D*, we amplified *WFZP-D* in the cDNA of both parents even though *WFZP-D* is not in the interval of *QSS.sicau-2D*. The results showed that *WFZP-D* had no sequence difference between YP and CS. Furthermore, there was no significant difference ($P > 0.05$) in the expression of *WFZP-D* in YP and CS by RT-qPCR analysis (Figure S4). One SNP was identified between CS and YP 60 bp downstream of the *WFZP-D* and a KASP marker named D21 was developed to assay the polymorphism. The D21 marker was mapped 9.4 cM away from *QSS.sicau-2D* in the reconstructed genetic map (Figure S5). These results indicated the *WFZP-D* is not the candidate gene for *QSS.sicau-2D*.

Eight spikelet/grain specific expressed genes were identified in the *QSS.sicau-2D* region, among which, one SNP converts the codon (TAT) to a translational stop codon (TAA) of *TraesCS2D03G0260700* in YP by exome sequencing and Sanger sequencing analysis. In addition, *TraesCS2D03G0260700* encoding cyclin-like F-box domain protein, and previous studies have shown that cyclin-like F-box domain is specifically expressed in wheat inflorescence and involved in the development of wheat inflorescence [61–65]. Overall, *TraesCS2D03G0260700* was predicted to be a potential candidate gene for *QSS.sicau-2D*.

Effects of *QSS.sicau-2 A* and *QSS.sicau-2D* on yield-related traits

Consistent with previous studies, GL, GW and TGW have decreased while GNS has increased, with the increase of SNS (Fig. 5), such as a single mutation in *WFZP-D* can significantly increase the SNS and GNS [49, 58, 59]. GWS is an important trait influencing wheat yield [66]. In this study, we found that the GWS exhibited a significant increase in YC population when *QSS.sicau-2 A* and *QSS.sicau-2D* coexisted. This may be attributed to the compensatory increase in grain number per spike (GNS) offsetting the decrease in thousand-grain weight (TGW). In conclusion, the SS trait have the value of increasing the yield potential of wheat.

Conclusion

In this study, two major SS QTL were identified in multi-environments and validated in different genetic populations. *QSS.sicau-2D* is a new QTL of SS trait, and predicted *TraesCS2D03G0260700* to be its candidate gene. At the same time, the combined effect of *QSS.sicau-2 A* and *QSS.sicau-2D* significantly increased GWS, which has the application value of increasing the yield potential of wheat.

Supplementary Information

The online version contains supplementary material available at <https://doi.org/10.1186/s12864-024-10540-7>.

Supplementary Material 1

Supplementary Material 2

Acknowledgements

Not applicable.

Author contributions

YXL designed and supervised the project. ZQW and HJL performed most of the experiments, with the assistance of XJZ, YZM, YZ, LY and XDC. FWK, HZ, YL and CXL participated in data analysis. ZQW drafted the manuscript and revised by YXL. All authors read and approved the final manuscript for publication.

Funding

This study was funded by the Key Program of Sichuan Natural Science Foundation (2022NSFSC0015), the Key Research of State Key Laboratory of Crop Gene Exploration and Utilization in Southwest China (SKL-KF202212) and the Research of State Key Laboratory of Crop Gene Exploration and Utilization in Southwest China (SKL-ZY202231).

Data availability

The datasets generated during the current study are available at the National Center for Biotechnology Information (NCBI) SRA repository under accession number PRJNA1041571.

Declarations

Ethics approval and consent to participate

No specific permit is required for the samples in this study. We comply with relevant institutional, national, and international guidelines and legislation for plant studies.

Consent for publication

Not applicable.

Competing interests

The authors declare no competing interests.

Received: 19 March 2024 / Accepted: 19 June 2024

Published online: 08 July 2024

References

- Ji GS, Xu ZB, Fan XL, Zhou Q, Yu Q, Liu XF, et al. Identification of a major and stable QTL on chromosome 5A confers spike length in wheat (*Triticum aestivum* L). *Mol Breeding*. 2021;41:1–13.
- Ji GS, Xu ZB, Fan XL, Zhou Q, Chen LG, Yu Q, et al. Identification and validation of major QTL for grain size and weight in bread wheat (*Triticum aestivum* L). *Crop J*. 2023;11(2):564–72.
- Simmonds J, Scott P, Leverington-Waite M, Turner AS, Brinton J, Korzun V, et al. Identification and independent validation of a stable yield and thousand grain weight QTL on chromosome 6A of hexaploid wheat (*Triticum aestivum* L). *BMC Plant Biol*. 2014;14:1–13.
- Ikeda K, Ito M, Nagasawa N, Kyojuka J, Nagato Y. Rice ABERRANT PANICLE ORGANIZATION 1, encoding an F-box protein, regulates meristem fate. *Plant J*. 2007;51(6):1030–40.
- Wolde GM, Trautewig C, Mascher M, Schnurbusch T. Genetic insights into morphometric inflorescence traits of wheat. *Theor Appl Genet*. 2019;132:1661–76.
- Liu HY, Wang K, Tang HL, Gong Q, Du LP, Pei XW, et al. CRISPR/Cas9 editing of wheat *TaQ* genes alters spike morphogenesis and grain threshability. *J Genet Genomics*. 2020;479:563–75.
- Coen ES, Nugent JM. Evolution of flowers and inflorescences *Development*, 1994 (Supplement): 107–16.
- Poursarebani N, Seidensticker T, Koppolu R, Trautewig C, Gawronski P, Bini F, et al. The genetic basis of composite spike form in barley and 'Miracle-Wheat'. *Genetics*. 2015;201(1):155–65.
- Zhu Y, Wagner D. Plant inflorescence architecture: The formation, activity, and fate of axillary meristems *Cold Spring Harbor perspectives in biology*. 2020;12(1):a034652.
- Yen C, Zheng YL, Yang JL. An ideotype for high yield breeding in theory and practice. *Proceedings of the 8th International Wheat Genetics Symposium*, Beijing, China. Edited by ZS Li and ZY Xin. 1993;(pp: 1113–1118).
- Rajaram S. Prospects and promise of wheat breeding in the 21st century. *Euphytica*. 2001;119(1–2):3–15.
- Peng ZS, Song XH, Zhang M. Cytogenetic studies on supernumerary spikelet wheat. *Seed*. 2000;(03): 3–6.
- Ma ZQ, Zhao DM, Zhang CQ, Zhang ZZ, Xue SL, Lin F, et al. Molecular genetic analysis of five spike-related traits in wheat using RIL and immortalized F₂ populations. *Mol Genet Genomics*. 2007;277:31–42.
- Chen ZY, Cheng XJ, Chai LL, Wang ZH, Du DJ, Wang ZH, et al. Pleiotropic QTL influencing spikelet number and heading date in common wheat (*Triticum aestivum* L). *Theor Appl Genet*. 2020;133:1825–38.
- Cui F, Ding AM, Li J, Zhao CH, Wang L, Wang XQ, et al. QTL detection of seven spike-related traits and their genetic correlations in wheat using two related RIL populations. *Euphytica*. 2012;186:177–92.
- Zhai HJ, Feng ZY, Li J, Liu XY, Xiao SH, Ni ZF, et al. QTL analysis of spike morphological traits and plant height in winter wheat (*Triticum aestivum* L.) using a high-density SNP and SSR-based linkage map. *Front Plant Sci*. 2016;7:1617.
- Zhou YP, Conway B, Miller D, Marshall D, Cooper A, Murphy P, et al. Quantitative trait loci mapping for spike characteristics in hexaploidy wheat. *Plant Genome*. 2017;10(2):plantgenome2016–10.
- Liu K, Sun XX, Ning TY, Duan XX, Wang QL, Liu TT, et al. Genetic dissection of wheat panicle traits using linkage analysis and a genome-wide association study. *Theor Appl Genet*. 2018;131:1073–90.
- Li G, Kuijter HNJ, Yang XJ, Liu HR, Shen CQ, Shi J, et al. MADS1 maintains barley spike morphology at high ambient temperatures. *Nat Plants*. 2021;78:1093–107.
- Ikeda K, Maekawa M, Izawa T, Itoh JI, Nagato Y. ABERRANT PANICLE ORGANIZATION 2/RFL, the rice ortholog of Arabidopsis LEAFY, suppresses the transition from inflorescence meristem to floral meristem through interaction with APO1. *Plant J*. 2012;69:168–80.

21. Yoshida A, Sasao M, Yasuno N, Takagi K, Daimon Y, Chen RH, et al. TAWAWA1, a regulator of rice inflorescence architecture, functions through the suppression of meristem phase transition. *Proc Natl Acad Sci*. 2013;110(2):767–72.
22. Dobrovolskaya O, Pont C, Sibout R, Martinek P, Badaeva E. FRIZZY PANICLE drives supernumerary spikelets in bread wheat. *Plant Physiol*. 2015;167:189–99.
23. James B, Adrian T, Simon G, John W, Snape DA, Laurie. A pseudo-response regulator is misexpressed in the photoperiod insensitive *Ppd-D1a* mutant of wheat (*Triticum aestivum* L). *Theor Appl Genet*. 2007;115:721–33.
24. Shaw LM, Bo L, Turner R, Li C, Dubcovsky J. *FLOWERING LOCUS T2 (FT2)* regulates spike development and fertility in temperate cereals. *J Exp Bot*. 2019;70(1):193–204.
25. Kuzay S, Xu YF, Zhang JL, Katz A, Pearce S, Su ZQ, et al. Identification of a candidate gene for a QTL for spikelet number per spike on wheat chromosome arm 7AL by high-resolution genetic mapping. *Theor Appl Genet*. 2019;132:2689–705.
26. Greenwood JR, Finnegan EJ, Watanabe N, Trevaskis B, Swain SM. New alleles of the wheat domestication gene *Q* reveal multiple roles in growth and reproductive development. *Development*. 2017;144:1959–65.
27. Sakuma S, Golan G, Guo ZF, Ogawa T, Tagiri A, Sugimoto K et al. Unleashing floret fertility in wheat through the mutation of a homeobox gene. *Proceedings of the National Academy of Sciences*. 2019;116(11):5182–5187.
28. Peng ZS, Yen C, Yang JL. Genetic control of supernumerary spikelet in common wheat line LYB. *Wheat Inform Service*. 1998;86:6–12.
29. Peng ZS, Yen C, Yang JL. Chromosomal location of genes for supernumerary spikelet in bread wheat. *Euphytica*. 1998;103:109–14.
30. Smith SE, Kuehl RO, Ray IM, Hui R, Soleri D. Evaluation of simple methods for estimating broad-sense heritability in stands of randomly planted genotypes. *Crop Sci*. 1998;38(5):1125–9.
31. Lei L, Zheng HL, Bi YL, Yang LM, Liu HL, Wang JG, et al. Identification of a major QTL and candidate gene analysis of salt tolerance at the bud burst stage in rice (*Oryza sativa* L.) using QTL-Seq and RNA-Seq. *Rice*. 2020;13:1–14.
32. Allen GC, Flores-Vergara MA, Krasynanski S, Kumar S, Thompson WF. A modified protocol for rapid DNA isolation from plant tissues using cetyltrimethylammonium bromide. *Nat Protoc*. 2006;1(5):2320–5.
33. Saghai-Marooof MA, Soliman KM, Jorgensen RA, Allard RW. Ribosomal DNA spacer-length polymorphisms in barley: mendelian inheritance, chromosomal location, and population dynamics. *Proceedings of the National Academy of Sciences*. 1984;81(24):8014–8018.
34. Yu Q, Feng B, Xu ZB, Fan XL, Zhou Q, Ji GS, et al. Genetic dissection of Three Major Quantitative Trait Loci for Spike Compactness and length in Bread Wheat (*Triticum aestivum* L). *Front Plant Sci*. 2022;13:882655.
35. Guo ZF, Yang QN, Huang FF, Zheng HJ, Sang ZQ, Xu YF et al. Development of high-resolution multiple-SNP arrays for genetic analyses and molecular breeding through genotyping by target sequencing and liquid chip. *Plant Commun*. 2021;2(6).
36. Zhu TT, Wang L, Rimplert H, Rodriguez JC, Deal KR, Oliveria RD, et al. Optical maps refine the bread wheat *Triticum aestivum* Cv. Chinese spring genome assembly. *Plant J*. 2021;107(1):303–14.
37. Danecek P, Stephan S, Richard D. Multiallelic calling model in bcftools (-m). 2014.
38. Wang K, Li MY, Hakonarson H. ANNOVAR: functional annotation of genetic variants from high-throughput sequencing data. *Nucleic Acids Res*. 2010;38(16):e164–164.
39. Abe A, Kosugi S, Yoshida K, Natsume S, Takagi H, Kanzaki H, et al. Genome sequencing reveals agronomically important loci in rice using MutMap. *Nat Biotechnol*. 2012;30:174–8.
40. Hill JT, Demarest BL, Bisgrove BW, Gorski B, Su YC, Yost HJ. MMAPP: mutation mapping analysis pipeline for pooled RNA-seq. *Genome Res*. 2013;23:687–97.
41. Takagi H, Abe A, Yoshida K, Kosugi S, Natsume S, Mitsuoka C, et al. QTL-seq: rapid mapping of quantitative trait loci in rice by whole genome resequencing of DNA from two bulked populations. *Plant J*. 2013;74(1):174–83.
42. Li CL, Ling FL, Su GH, Sun WF, Liu HS, Su YC, et al. Location and mapping of the NCLB resistance genes in maize by bulked segregant analysis (BSA) using whole genome re-sequencing. *Mol Breeding*. 2020;40:1–12.
43. Han YH, Khu DM, Monteros MJ. High-resolution melting analysis for SNP genotyping and mapping in tetraploid alfalfa (*Medicago sativa* L). *Mol Breeding*. 2019;29:489–501.
44. Tan CT, Yu HJ, Yang Y, Xu XY, Chen MS, Rudd JC, et al. Development and validation of KASP markers for the greenbug resistance gene *Gb7* and the hessian fly resistance gene *H32* in wheat. *Theor Appl Genet*. 2017;130:1867–84.
45. Van Ooijen JW. Software for the calculation of genetic linkage maps in experimental populations Kyazma BV. Wageningen, Netherlands. 2006.
46. Van Ooijen JW. MapQTL version 5.0, software for the map-ping of quantitative trait loci in experimental populations. Wageningen: Kyazma BV; 2004.
47. Chen A, Kong L. CGPS: a machine learning-based approach integrating multiple gene set analysis tools for better prioritization of biologically relevant pathways. *J Genet Genomics*. 2018;45:489–504.
48. Luo W, Zhou JG, Liu JJ, Liu YL, Mu Y, Tang HP, et al. Fine mapping of the *hairy glume (hg)* gene in a chromosome variation region at the distal terminus of 1AS. *Front Plant Sci*. 2012;13:1006510.
49. Du DJ, Zhang DX, Yuan J, Feng M, Li ZJ, Wang ZH, et al. FRIZZY PANICLE defines a regulatory hub for simultaneously controlling spikelet formation and awn elongation in bread wheat. *New Phytol*. 2021;231:814–33.
50. Reynolds MP, Rajaram S, Sayre KD. Physiological and genetic changes of irrigated wheat in the post-green revolution period and approaches for meeting projected global demand. *Crop Sci*. 1999;39(6):1611–21.
51. PENNELL A, Halloran GM. Influence of vernalization and photoperiod on supernumerary spikelet expression in wheat. *Ann Botany*. 1984;53(6):821–31.
52. Swaminathan MS, Chopra VL, Sastry GRK. Expression and stability of an induced mutation for ear branching in bread wheat. *Curr Sci*. 1966;35(4):91–2.
53. Katz A, Byrne P, Reid S, Bratschun S, Haley S, Pearce S. Identification and validation of a QTL for spikelet number on chromosome arm 6BL of common wheat (*Triticum aestivum* L). *Mol Breeding*. 2022;42(4):17.
54. Jiang C, Xu ZB, Fan XL, Zhou Q, Ji GS, Chen LG, et al. Identification and validation of quantitative trait loci for fertile spikelet number per spike and grain number per fertile spikelet in bread wheat (*Triticum aestivum* L). *Theor Appl Genet*. 2023;136(4):69.
55. Kuang CH, Zhao XF, Yang K, Zhang ZP, Ding L, Pu ZE, et al. Mapping and characterization of major QTL for spike traits in common wheat. *Physiol Mol Biology Plants*. 2020;26:1295–307.
56. Koppolu R, Schnurbusch T. Developmental pathways for shaping spike inflorescence architecture in barley and wheat. *J Integr Plant Biol*. 2019;61(3):278–95.
57. Hu WJ, Zhu DM, Zhang Y, Liu J, Zhao D, Liao S, et al. Quantitative trait loci mapping for heading date and spikelet number in wheat (*Triticum aestivum* L.) based on two recombinant inbred line populations. *Genet Resour Crop Evol*. 2023;70:1179–95.
58. Li YP, Li L, Zhao MC, Guo L, Guo XX, Zhao D, et al. Wheat FRIZZY PANICLE activates *VERNALIZATION1-A* and *HOMEBOX4-A* to regulate spike development in wheat. *Plant Biotechnol J*. 2021;19(6):1141–54.
59. Ma J, Ding PY, Liu JJ, Li T, Zou YY, Habib A, et al. Identification and validation of a major and stably expressed QTL for spikelet number per spike in bread wheat. *Theor Appl Genet*. 2019;132:3155–67.
60. Dobrovolskaya O, Martinek P, Voylovok AV, Korzun V, Röder MS, Börner A. Microsatellite mapping of genes that determine supernumerary spikelets in wheat (*T. aestivum*) and rye (*S. cereale*). *Theoretical and applied genetics*. 2009;119:867–874.
61. Hong MJ, Kim JB, Seo YW, Kim DY. F-box genes in the wheat genome and expression profiling in wheat at different developmental stages. *Genes*. 2020;11:1154.
62. Li HY, Wei CR, Meng YY, Fan RQ, Zhao WQ, Wang XD, et al. Identification and expression analysis of some wheat F-box subfamilies during plant development and infection by *Puccinia Triticina*. *Plant Physiol Biochem*. 2020;155:535–48.
63. Kipreos ET, Pagano M. The F-box protein family. *Genome Biol*. 2000;1:1–7.
64. Zhang XB, Gonzalez-Carranza ZH, Zhang SL, Miao YC, Liu CJ, Roberts JA. F-Box proteins in plants. *Annu Plant Rev*. 2019;2:307–28.
65. Hong MJ, Kim DY, Kang SY, Kim DS, Kim JB, Seo YW. Wheat F-box protein recruits proteins and regulates their abundance during wheat spike development. *Mol Biol Rep*. 2012;39:9681–96.
66. Protich R, Todorovich G, Protich N. Grain weight per spike of wheat using different ways of seed protection. *Bulgarian J Agricultural Sci*. 2012;18(2):185–90.

Publisher's Note

Springer Nature remains neutral with regard to jurisdictional claims in published maps and institutional affiliations.